T_{FH} cells depend on Tcf1-intrinsic HDAC activity to suppress CTLA4 and guard B-cell help function

Fengyin Li[a,b,1,2], Xin Zhao[c,1], Yali Zhang[d], Peng Shao[e], Xiaoke Ma[f], William J. Paradee[g], Chengyu Liu[h], Jianmin Wang[d,2], and Hai-Hui Xue[c,e,i,2]

[a]Department of Rheumatology and Immunology, the First Affiliated Hospital of USTC, Division of Life Sciences and Medicine, University of Science and Technology of China, 230001 Hefei, Anhui, People's Republic of China; [b]Hefei National Laboratory for Physical Sciences at Microscale, the Chinese Academy of Sciences Key Laboratory of Innate Immunity and Chronic Disease, School of Basic Medical Sciences, Division of Life Sciences and Medicine, University of Science and Technology of China, 230027 Hefei, Anhui, People's Republic of China; [c]Center for Discovery and Innovation, Hackensack University Medical Center, Nutley, NJ 07110; [d]Department of Biostatistics and Bioinformatics, Roswell Park Comprehensive Cancer Center, Buffalo, NY 14263; [e]Department of Microbiology and Immunology, Carver College of Medicine, University of Iowa, Iowa City, IA 52242; [f]School of Computer Science and Technology, Xidian University, 215123 Xi'an, Shanxi, People's Republic of China; [g]Genome Editing Core Facility, University of Iowa, Coralville, IA 52241; [h]Transgenic Core Facility, National Heart, Lung, and Blood Institute, National Institutes of Health, Bethesda, MD 20892; and [i]Immunology Research Laboratory, New Jersey Veterans Affairs Health Care System, East Orange, NJ 07018

Edited by Kenneth M. Murphy, Washington University in St. Louis School of Medicine, St. Louis, MO, and approved October 30, 2020 (received for review July 10, 2020)

Precise regulation of coinhibitory receptors is essential for maintaining immune tolerance without interfering with protective immunity, yet the mechanism underlying such a balanced act remains poorly understood. In response to protein immunization, T follicular helper (T_{FH}) cells lacking Tcf1 and Lef1 transcription factors were phenotypically normal but failed to promote germinal center formation and antibody production. Transcriptomic profiling revealed that Tcf1/Lef1-deficient T_{FH} cells aberrantly upregulated CTLA4 and LAG3 expression, and treatment with anti-CTLA4 alone or combined with anti-LAG3 substantially rectified B-cell help defects by Tcf1/Lef1-deficient T_{FH} cells. Mechanistically, Tcf1 and Lef1 restrain chromatin accessibility at the *Ctla4* and *Lag3* loci. Groucho/Tle corepressors, which are known to cooperate with Tcf/Lef factors, were essential for T_{FH} cell expansion but dispensable for repressing coinhibitory receptors. In contrast, mutating key amino acids in histone deacetylase (HDAC) domain in Tcf1 resulted in CTLA4 derepression in T_{FH} cells. These findings demonstrate that Tcf1-instrinsic HDAC activity is necessary for preventing excessive CTLA4 induction in protein immunization–elicited T_{FH} cells and hence guarding their B-cell help function.

follicular helper T cells | transcriptional regulation | coinhibitory pathway

Coinhibitory receptors, such as CTLA4, LAG3 and PD1, provide essential counterbalance to stimulatory signals in T cells to maintain tolerance and prevent autoimmunity (1, 2). On the other hand, excessive activation of coinhibitory pathways in chronic microbial infections and tumor microenvironments impedes eradication of microbes and transformed cells (3, 4). Precise control of coinhibitory receptor expression is therefore pivotal to achieve protective immunity while avoiding tissue damage. B cell responses are stimulated by T follicular helper (T_{FH}) cells but restrained by regulatory T (T_{REG}) and T follicular regulatory (T_{FR}) cells, and CTLA4 exerts critical regulatory roles in this process through both cell-intrinsic and cell-extrinsic mechanisms (5–8). While CTLA4 is constitutively expressed in T_{REG} cells, it is not expressed in conventional naïve $CD4^+$ T cells but is induced upon activation (7). Induced deletion of CTLA4 in T_{FH} cells modestly enhances the stimulatory effect on B cells in vitro (5), while forced expression of CTLA4 in T_{FH} cells substantially compromises generation of germinal center (GC)-B cells in vivo (9). It is clear that fine-tuning CTLA4 expression in T_{FH} cells is critical for optimal B-cell help function, yet the underlying mechanisms are not fully understood.

Tcf1 and Lef1 transcriptional factors (TFs) have versatile functions in T cells, ranging from early T cell development in the thymus to mature T cell responses in the periphery (10, 11). In $CD4^+$ T cells, Tcf1 promotes T_H2 but antagonizes T_H1 and T_H17 differentiation (12, 13). Recently, we and others demonstrated that although Tcf1 and Lef1 are expressed at lower levels in T_{REG} cells than in conventional $CD4^+$ T cells, they are necessary for the immunosuppressive function of T_{REG} cells (14, 15). Furthermore, Foxp3-Cre–mediated ablation of Tcf1 and Lef1 greatly diminished generation of spontaneous T_{FR} cells under homeostatic state (15). In T_{FH} cells elicited by acute infection with lymphocytic choriomeningitis virus (LCMV-) Armstrong strain, Tcf1 is required for induction of Bcl6, the T_{FH}-lineage defining TF, and optimal expression of Icos costimulatory receptor and IL-6 receptor to fully activate the T_{FH} transcriptional program (16–18). However, it is also noted that Tcf1 does not seem to be necessary for T_{FH} responses during protein immunization with alum as an adjuvant (18). It remains unknown if the discrepancy in a requirement for T_{FH} cells is due to a compensatory effect by Lef1 or because Tcf1 and Lef1 control different aspects of T_{FH} cell differentiation in response to protein immunization.

Tcf/Lef TFs act as transcriptional activators or repressors, depending on the interacting partners, gene, and cell context.

Significance

A successful vaccine depends on productive T follicular helper (T_{FH}) and B-cell responses to elicit protective immunity. Vaccines are delivered as live-attenuated viruses, inactivated organisms, or protein subcomponents via different routes. In the context of protein immunization, we demonstrate that Tcf1 and Lef1 transcription factors play critical roles in suppressing excessive induction of CTLA4 and LAG3 coinhibitory receptors in T_{FH} cells and, hence, preventing undue inhibition of B cells. This function is in contrast to the requirement for Tcf1 and Lef1 in induction of Bcl6 in T_{FH} cells elicited by viral or bacterial infections. These findings highlight that the same protein factors could be utilized to regulate distinct aspects of T_{FH} cell differentiation depending on vaccination routes and regimens.

Author contributions: F.L. and H.-H.X. designed research; F.L., X.Z., P.S., X.M., W.J.P., and C.L. performed research; W.J.P. and C.L. contributed new reagents/analytic tools; F.L., X.Z., Y.Z., P.S., X.M., J.W., and H.-H.X. analyzed data; and F.L., J.W., and H.-H.X. wrote the paper.

The authors declare no competing interest.

This article is a PNAS Direct Submission.

[1]F.L. and X.Z. contributed equally to this work.

[2]To whom correspondence may be addressed. Email: fyli88@ustc.edu.cn, jianmin.wang@roswellpark.org, or haihui.xue@hmh-cdi.org.

This article contains supporting information online at https://www.pnas.org/lookup/suppl/doi:10.1073/pnas.2014562118/-/DCSupplemental.

Published December 28, 2020.

β-catenin is a known coactivator for Tcf/Lef TFs but appears to be dispensable for activating Bcl6 transcription in infection-elicited T_{FH} (Inf_T_{FH}) cells because ablation of β-catenin alone, or together with its homolog γ-catenin, or Tcf1 long isoforms, of which the N termini are responsible for β-catenin interaction, did not affect Bcl6 induction (19, 20). Our recent study reveals that Ezh2, in its Ser21-phosphorylated form, functions as a coactivator with Tcf1 to induce Bcl6 in Inf_T_{FH} cells (21). As for target gene

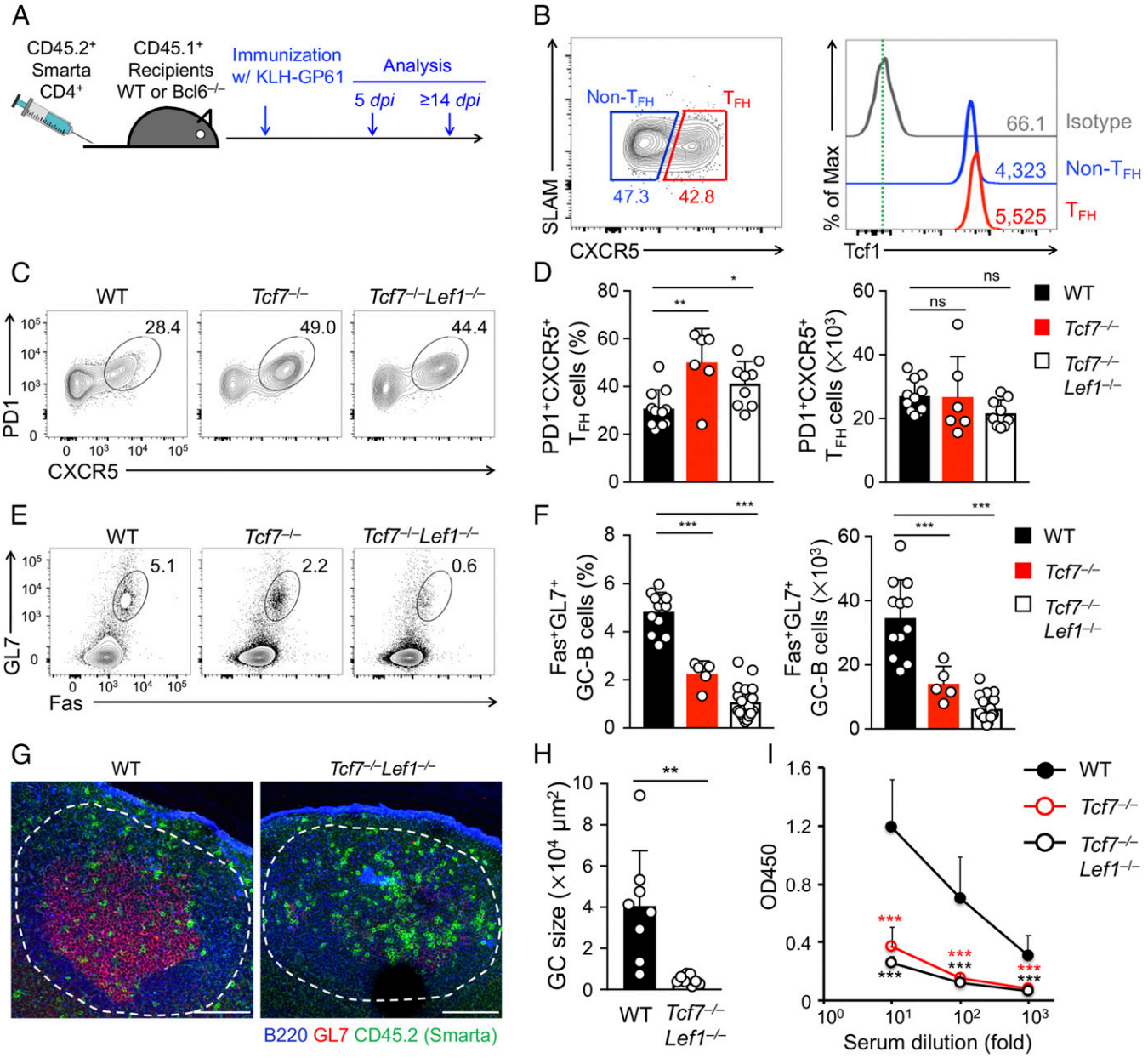

Fig. 1. Tcf1 and Lef1 are required for B-cell help function by T_{FH} cells elicited by protein immunization. (*A*) Experimental design. WT (1×10^5) or *Tcf7*$^{-/-}$ or *Tcf7*$^{-/-}$*Lef1*$^{-/-}$ (2×10^5) Smarta CD4$^+$ T cells were adoptively transferred into CD45.1$^+$ WT or *Bcl6*$^{-/-}$ B6.SJL recipients, which were immunized with KLH-GP61 24 h later. T_{FH} and GC-B cell responses were examined on day 5 and ≥14 postimmunization, respectively. (*B*) The detection of Tcf1 expression in T_{FH} and non-T_{FH} cells was derived from WT Smarta CD4$^+$ T cells in dLNs on day 5 postimmunization. The values in the contour plot denote percentage, and those in histogram denote geometric mean fluorescence intensity. (*C* and *D*) The detection of CXCR5$^+$PD1$^+$ T_{FH} cells in CD45.2$^+$GFP$^+$ Smarta cells in dLNs of WT recipients on day 5 postimmunization. Representative contour plots are from two to three independent experiments (*C*). Cumulative data on T_{FH} cell frequency (*Left*) and numbers (*Right*) are means ± SD (*D*). (*E* and *F*) The detection of Fas$^+$GL7$^+$ GC-B cells in B220$^+$CD19$^+$ B cells in dLNs of *Bcl6*$^{-/-}$ recipients on day 14 postimmunization. Representative contour plots are from two to three independent experiments (*E*), and cumulative data on GC-B cell frequency (*Left*) and numbers (*Right*) are means ± SD (*F*). (*G*) The detection of B cell follicle (blue), GC (red), and Smarta CD4$^+$ T cells (green) by immunofluorescence staining of dLNs from *Bcl6*$^{-/-}$ recipients on day 14 postimmunization. (Scale bars, 100 μm.) Data are representative from three experiments. (*H*) The cumulative data on GC sizes from at least two independent experiments, with ≥2 LN sections measured for each genotype. Note that in recipients of *Tcf7*$^{-/-}$*Lef1*$^{-/-}$ Smarta cells, well-structured GCs are rarely observed, and instead, areas of GL7$^+$ cell aggregates were measured. (*I*) The detection of KLH-specific IgG in sera of *Bcl6*$^{-/-}$ recipients on day 14 postimmunization. The data are from two experiments ($n = 4$ to 6). OD450, optical density at 450 nm. Statistical significance was first determined with one-way ANOVA for multigroup comparison, and as post hoc correction, Tukey's test was used for indicated pair-wise comparison. *$P < 0.05$; **$P < 0.01$; ***$P < 0.001$; ns, not statistically significant.

repression, Groucho/Tle proteins are known corepressors that interact with Tcf/Lef TFs (22, 23). Among four Tle genes that encode full-length Grouch/Tle proteins in mammals, Tle3 is most abundantly expressed in T cells, with Tle4 detected at intermediate and Tle1 and Tle2 at low levels (24). Tle genes exhibit strong functional redundancy and gene dosage dependency, as observed in late stages of thymic development, where deleting *Tle3* along with at least one allele each of *Tle1* and *Tle4* is necessary to abrogate $CD8^+$ T cell production (24). We previously discovered that Tcf1 and Lef1 have intrinsic histone deacetylase (HDAC) activity, which is responsible for repressing $CD4^+$ lineage-associated genes in $CD8^+$ lineage-committed thymocytes (25). It remained unknown if Tle corepressors have a role in T_{FH} cell differentiation and if Tcf1/Lef1 HDAC activity contributes to immune regulation beyond their role in establishing $CD8^+$ T cell identity during thymic development.

To address these critical knowledge gaps, we adopted a protein immunization method to elicit T_{FH} cell responses and used mouse models developed in this work to address the functional redundancy between Tcf1 and Lef1, requirements for Tcf1 HDAC activity, and roles of Tle1 to 4 corepressors in immunization-elicited T_{FH} (Imm_T_{FH}) cells. This systematic approach revealed that Tcf1 and Lef1 were essential for restraining CTLA4 and LAG3 expression in Imm_T_{FH} cells and thus protecting them from undue inhibition of GC-B cell responses. The repression of CTLA4 required Tcf1 HDAC activity but did not depend on Tle corepressors, whereas loss of Tle proteins impaired proliferation of activated $CD4^+$ T cells and hence production of T_{FH} cells.

Results

Tcf1/Lef1-Deficient Imm_T_{FH} Cells Are Phenotypically Normal but Functionally Impaired. Tcf1 and Lef1 are known to have redundant functions, with Tcf1 showing a more predominant regulatory effect. As shown previously, in the process of establishing thymic $CD8^+$ T cell identity (25), generation of $CD8^+$ memory precursor cells (26), immunosuppressive function of regulatory T cells (14), and differentiation of Inf_T_{FH} (17), ablation of Lef1 alone shows little to modest impact, but loss of Lef1 exacerbates the more evident defects caused by Tcf1 deficiency. To evaluate if the lack of impact of Tcf1 ablation on Imm_T_{FH} cells (18) was due to compensation by Lef1, we used *hCD2-Cre* to ablate *Tcf7* and/or *Lef1* genes (encoding Tcf1 and Lef1, respectively) in mature T cells so as not to affect thymic development (10, 17). Preliminary studies showed that adoptively transferred *hCD2-Cre*$^+$ *Tcf7*$^{FL/FL}$ *Lef1*$^{FL/FL}$ (*Tcf7*$^{-/-}$*Lef1*$^{-/-}$) $CD4^+$ T cells homed to secondary lymphoid organs at ~50% efficiency of wild-type (WT) cells, with similar survival capability (*SI Appendix*, Fig. S1). We therefore transferred *Tcf7*$^{-/-}$ or *Tcf7*$^{-/-}$*Lef1*$^{-/-}$ Smarta $CD4^+$ T cells at 2-fold as many as WT Smarta cells in immunization experiments with keyhole limpet hemocyacin (KLH) conjugated with LCMV glycoprotein 61–80 peptides (KLH-GP61) (Fig. 1*A*) so that they were activated at similar precursor frequencies in the draining popliteal lymph nodes (dLNs). Tcf1 expression was similar between WT $CXCR5^+$ T_{FH} and $CXCR5^-$ non-T_{FH} cells on day 5 postimmunization (Fig. 1*B*) but was effectively ablated in *Tcf7*$^{-/-}$ or *Tcf7*$^{-/-}$*Lef1*$^{-/-}$ cells, as validated by intranuclear staining (*SI Appendix*, Fig. S2*A*). Unlike Inf_T_{FH} cells that are greatly diminished in the absence of Tcf1 and Lef1

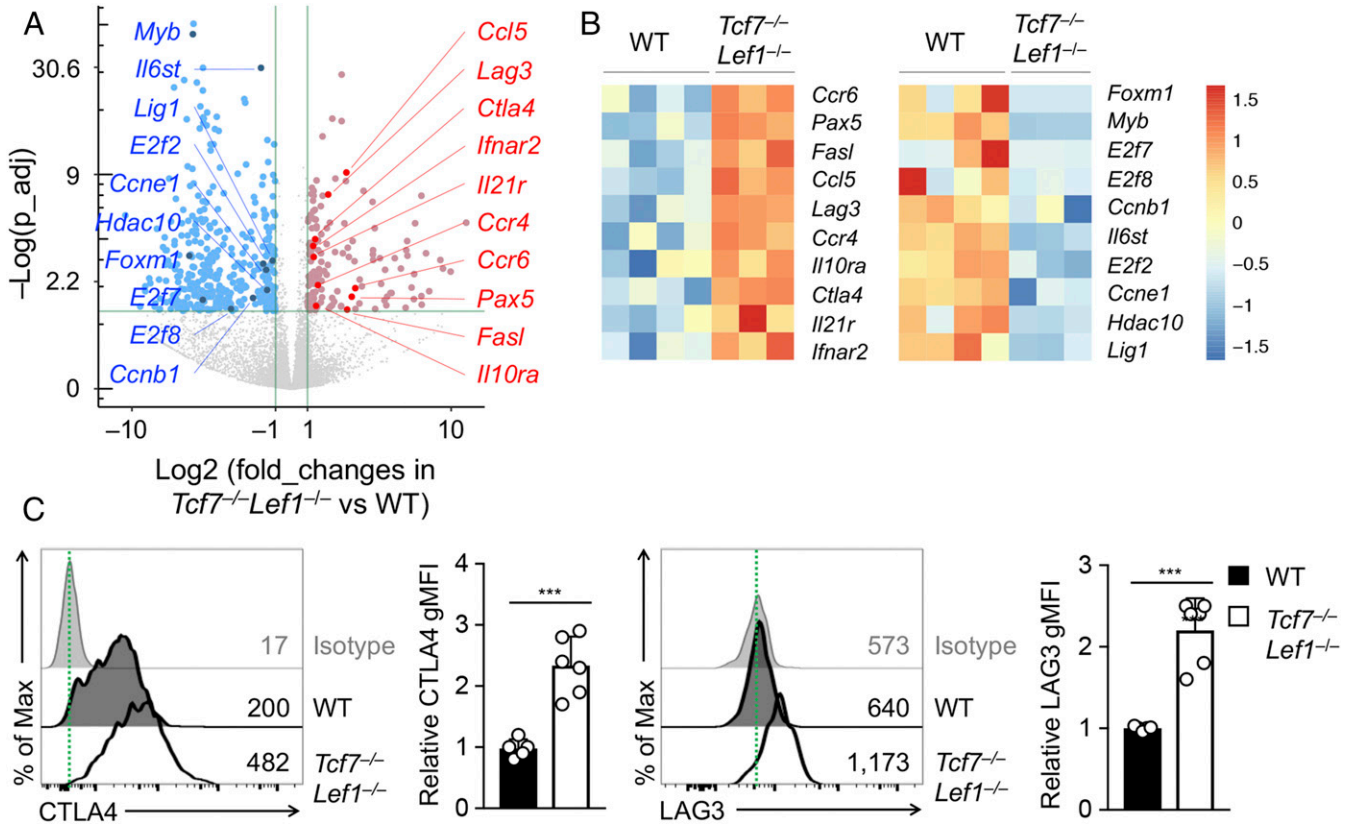

Fig. 2. Tcf1/Lef1 deficiency leads to aberrant up-regulation of coinhibitory receptors in Imm_T_{FH} cells. (*A*) A volcano plot showing differential gene expression between WT and Tcf1/Lef1-deficient Imm_T_{FH} cells, with select genes highlighted. (*B*) A heatmap showing relative expression of select genes in replicates of WT and Tcf1/Lef1-deficient Imm_T_{FH} cells. (*C*) The detection of CTLA4 and LAG3 proteins in WT and Tcf1/Lef1-deficient Imm_T_{FH} cells on day 5 postimmunization. In half-stacked histographs, the dotted vertical lines mark signal strength by isotype staining, and values denote geometric mean fluorescence intensity (gMFI). The bar graphs are means ± SD of relative gMFI from two experiments. ***$P < 0.001$.

(16–18, 27), similar numbers of CXCR5$^+$PD1$^+$ T_{FH} cells were detected in response to protein immunization in recipients of WT, *Tcf7*$^{-/-}$, or *Tcf7*$^{-/-}$*Lef1*$^{-/-}$ Smarta cells, albeit Tcf1- or Tcf1/Lef1-deficient T_{FH} cells were detected at modestly elevated frequency than WT T_{FH} cells (Fig. 1 *C* and *D*). Icos expression also showed a modest increase in *Tcf7*$^{-/-}$*Lef1*$^{-/-}$ T_{FH} cells than WT cells (*SI Appendix*, Fig. S2*B*). In addition, similar numbers of CXCR5$^+$Bcl6$^+$ germinal center T_{FH} (GC-T_{FH}) cells were observed among all genotypes, and Bcl6 expression levels were similar among WT, *Tcf7*$^{-/-}$, and *Tcf7*$^{-/-}$*Lef1*$^{-/-}$ T_{FH} cells (*SI*

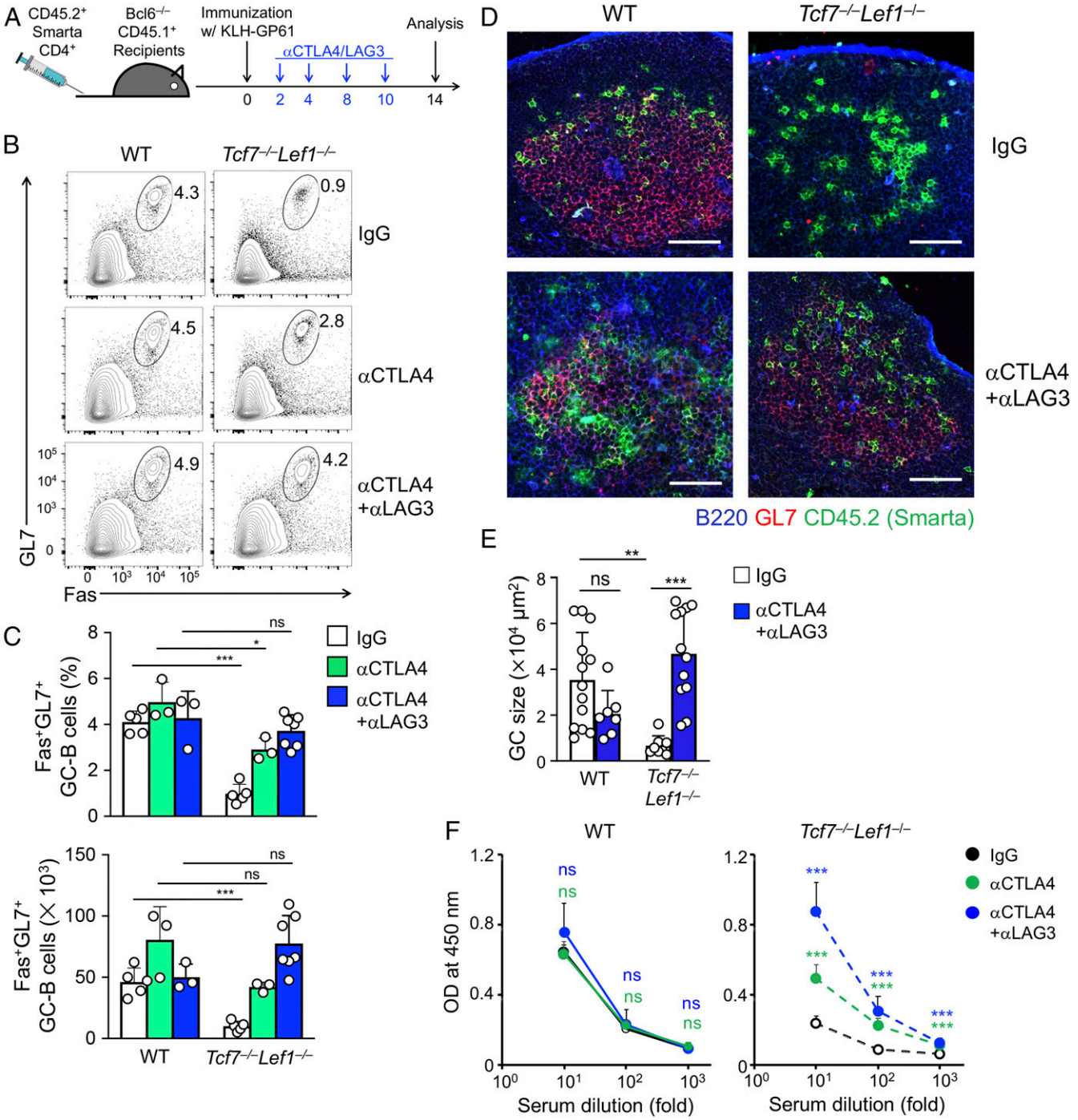

Fig. 3. Blocking CTLA4 and LAG3 restores B-cell help by Tcf1/Lef1-deficient T_{FH} cells. (*A*) The experimental design for treatment with anti-CTLA4 and/or anti-LAG3 antibodies, where WT (1×10^5) or *Tcf7*$^{-/-}$*Lef1*$^{-/-}$ (2×10^5) Smarta CD4$^+$ T cells were transferred. (*B* and *C*) The detection of GC-B cells in *Bcl6*$^{-/-}$ recipients on day 14 postimmunization. The representative contour plots in *B* show percentages of GC-B cells in B220$^+$CD19$^+$ B cells in dLNs from two independent experiments, and cumulative data on percentages and numbers of GC-B cells in *C* are means ± SD. (*D*) The detection of GC formation (red) by immunofluorescence staining of dLNs from *Bcl6*$^{-/-}$ recipients on day 14 postimmunization. (Scale bars, 100 μm.) Data are representative from two to three experiments. (*E*) Cumulative data on GC sizes from at least two independent experiments with ≥ 2 LN sections measured for each experimental condition. (*F*) The detection of KLH-specific IgG in sera of *Bcl6*$^{-/-}$ recipients on day 14 postimmunization. OD450, optical density at 450 nm. Data are from two experiments (n = 3 to 5). *$P < 0.05$; **$P < 0.01$; ***$P < 0.001$; ns, not statistically significant.

Appendix, Fig. S2 *C* and *D*). WT and *Tcf7*$^{-/-}$*Lef1*$^{-/-}$ Smarta CD4^{+} T cells were detected at similar frequency in B cell follicles in dLNs, as determined by immunofluorescence staining (*SI Appendix*, Fig. S2*E*). These data collectively indicate that Tcf1 and Lef1 are not required for generation of phenotypic Imm_T$_{FH}$ cells, their migration into B cell follicles, and the T$_{FH}$ lineage–defining Bcl6 expression. This is in key contrast to an indispensable role of Tcf1 and Lef1 in regulating these aspects in Inf_T$_{FH}$ cells.

We next investigated if the phenotypically "normal" *Tcf7*$^{-/-}$ and *Tcf7*$^{-/-}$*Lef1*$^{-/-}$ Imm_T$_{FH}$ cells were adequate in conferring B-cell help. To this end, we used CD45.1^{+} *Cd4Cre*$^{+}$ *Bcl6*$^{fl/fl}$ (called *Bcl6*$^{-/-}$ hereafter) mice as adoptive transfer recipients, where the endogenous T$_{FH}$ and T$_{FR}$ responses are abrogated but B cells remain functional (21). Following transfer of Smarta CD4^{+} T cells and KLH-GP61 immunization, we analyzed humoral responses in the recipients on day 14 postimmunization. The formation of Fas^{+}GL7^{+} GC-B cells was reduced in

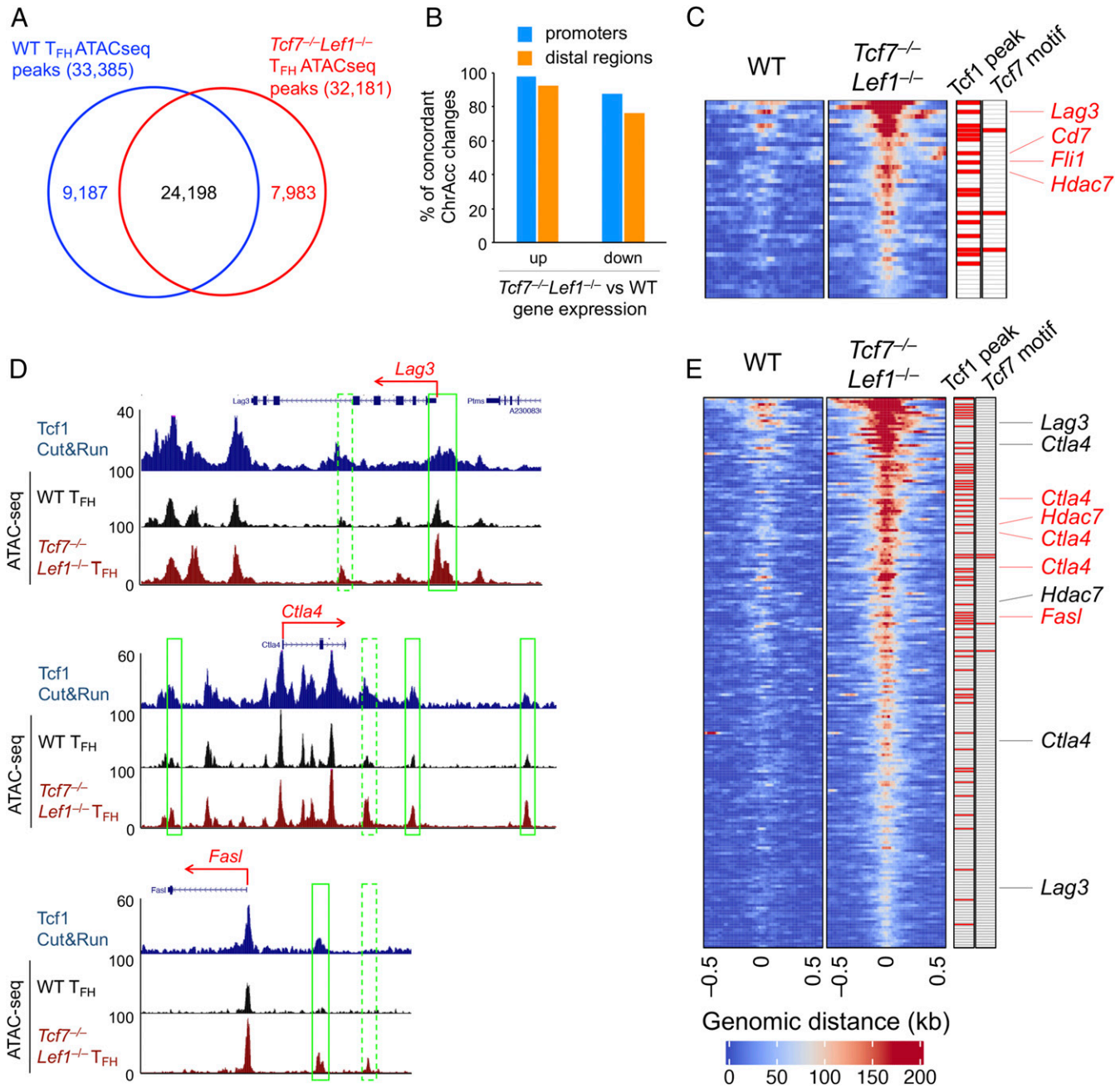

Fig. 4. Tcf1 and Lef1 negatively regulate *Ctla4* and *Lag3* by limiting chromatin accessibility. (*A*) Venn diagram showing differential chromatin accessibility between WT and Tcf1/Lef1-deficient T$_{FH}$ cells, as determined by ATAC-seq. (*B*) Bar graphs summarizing the percentage of ChrAcc sites that show an increase in up-regulated or decrease in down-regulated genes in Tcf1/Lef1-deficient T$_{FH}$ cells, at either promoters or distal regulatory regions. (*C*) Heatmaps showing increased ChrAcc at the promoters of up-regulated genes in Tcf1/Lef1-deficient T$_{FH}$ cells. The two columns on the right denote the presence of Tcf1-binding peaks and *Tcf7* motif with red lines. Select genes associated with increased ChrAcc are marked, with those in red denoting overlap with Tcf1 peak(s). (*D*) Tcf1 CUT&RUN track in WT T$_{FH}$ cells and ATAC-seq tracks of WT and Tcf1/Lef1-deficient T$_{FH}$ cells at select up-regulated gene loci. The structure and transcription direction are marked on top. The green rectangles mark increased ChrAcc sites Tcf1/Lef1-deficient T$_{FH}$ cells, with solid ones denoting overlap with Tcf1 peak(s). (*E*) Heatmaps showing increased ChrAcc at the distal regions of up-regulated genes in Tcf1/Lef1-deficient T$_{FH}$ cells as in *C*.

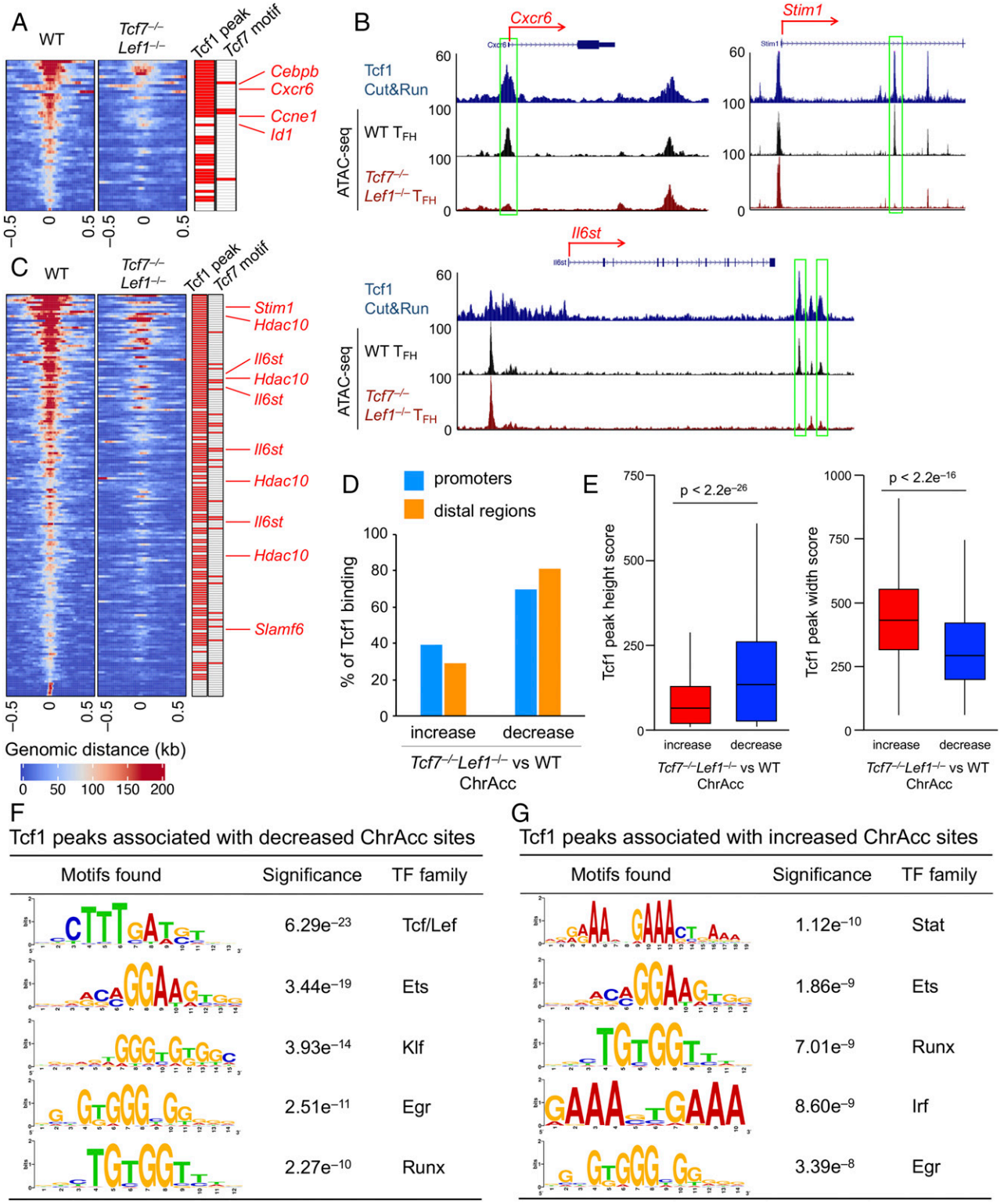

Fig. 5. Tcf1 and Lef1 positively regulate T_{FH} genes by maintaining a chromatin-accessible state. (*A*) Heatmaps showing decreased ChrAcc at the promoters of down-regulated genes in Tcf1/Lef1-deficient T_{FH} cells. The two columns on the right denote the presence of Tcf1-binding peaks and *Tcf7* motif with red lines. Select genes associated with decreased ChrAcc are marked, with those in red denoting an overlap with Tcf1 peak(s). (*B*) The Tcf1 CUT&RUN track in WT T_{FH} cells and ATAC-seq tracks of WT and Tcf1/Lef1-deficient T_{FH} cells at select down-regulated gene loci. The structure and transcription direction are marked on top. The green rectangles mark decreased ChrAcc sites, with solid ones denoting overlap with Tcf1 peak(s). (*C*) Heatmaps showing decreased ChrAcc at the distal regions of down-regulated genes in Tcf1/Lef1-deficient T_{FH} cells as in *A*. (*D*) A bar graph summarizing the frequency of Tcf1-binding to differential ChrAcc sites at promoters and distal regulatory regions between *Tcf7*$^{-/-}$*Lef1*$^{-/-}$ and WT T_{FH} cells. (*E*) Box plots showing Tcf1 peak heights (*Left*) or width (*Right*) associated with differential ChrAcc sites between *Tcf7*$^{-/-}$*Lef1*$^{-/-}$ and WT T_{FH} cells. The statistical significance is determined by Student's *t* test. (*F* and *G*) Motif analysis of Tcf1 peaks associated with decreased (*F*) or increased (*G*) ChrAcc sites in *Tcf7*$^{-/-}$*Lef1*$^{-/-}$ T_{FH} cells. The top five motifs of the transcription factor family are shown together with motif logos and statistical significance.

frequency and numbers in recipients of *Tcf7*$^{-/-}$ cells and were further diminished in those of *Tcf7*$^{-/-}$*Lef1*$^{-/-}$ cells (Fig. 1 *E* and *F*). In line with this observation, whereas highly structured GCs were detected in recipients of WT Smarta CD4^{+} T cells, only scattered GC-B cells were in follicles without clearly definable structures in recipients of *Tcf7*$^{-/-}$*Lef1*$^{-/-}$ cells (Fig. 1 *G* and *H*). In addition, KLH-specific antibodies were greatly diminished in recipients of *Tcf7*$^{-/-}$ or *Tcf7*$^{-/-}$*Lef1*$^{-/-}$ cells (Fig. 1*I*). These analyses suggest that Tcf1 and Lef1 are necessary for T_{FH} function as B-cell helpers but dispensable for T_{FH} differentiation in response to protein immunization.

Tcf1 and Lef1 Repress Coinhibitory Receptors in Imm_T_{FH} Cells. To determine the mechanistic requirements for Tcf1/Lef1 in Imm_T_{FH} cells, we performed RNA sequencing (RNA-seq) on WT and *Tcf7*$^{-/-}$*Lef1*$^{-/-}$ T_{FH} cells isolated on day 5 postimmunization, and the replicates in each genotype formed distinct clusters based on principal component analysis (*SI Appendix*, Fig. S3*A*). Global transcriptomic analysis with GSEA showed that the gene set enriched in Inf_T_{FH} cells (17) was negatively correlated in *Tcf7*$^{-/-}$*Lef1*$^{-/-}$ Imm_T_{FH} cells (*SI Appendix*, Fig. S3*B*), consistent with a known role of Tcf1 and Lef1 in inducing T_{FH} transcriptional program. In addition, Tcf1-activated and -repressed gene sets in Inf_T_{FH} cells (17) showed negative and positive enrichment in *Tcf7*$^{-/-}$*Lef1*$^{-/-}$ Imm_T_{FH} cells, respectively (*SI Appendix*, Fig. S3 *C* and *D*), indicating a substantial overlap of Tcf1/Lef1-dependent transcriptional programs between Inf_T_{FH} and Imm_T_{FH} cells. Gene set enrichment analysis (GSEA) also revealed positive enrichment of CTLA4 pathways and negative enrichment of cell cycles, E2F targets, and FOXM1 pathways in *Tcf7*$^{-/-}$*Lef1*$^{-/-}$ Imm_T_{FH} cells (*SI Appendix*, Fig. S3 *E–H*).

By the criteria of ≥2-fold expression changes and adjusted $P < 0.05$, 359 genes were down-regulated and 157 genes up-regulated in *Tcf7*$^{-/-}$*Lef1*$^{-/-}$ over WT Imm_T_{FH} cells. *Il6st* (encoding gp130) and *Myb* expression was diminished in *Tcf7*$^{-/-}$*Lef1*$^{-/-}$ Imm_T_{FH} cells (Fig. 2 *A* and *B*), exhibiting similar changes as those in Tcf1/Lef1-deficient Inf_T_{FH} cells (*SI Appendix*, Fig. S3*C*) (17). However, *Bcl6*, *Icos*, and *Pdcd1* were not among the down-regulated genes, and *Cxcr5* expression was modestly elevated, if at all, in *Tcf7*$^{-/-}$*Lef1*$^{-/-}$ Imm_T_{FH} cells (*SI Appendix*, Fig. S4*A*), in line with immunophenotypic analysis (*SI Appendix*, Fig. S2*A*). On the other hand, *Lag3*, *Ccl5,* and *Ccr6* were up-regulated in *Tcf7*$^{-/-}$*Lef1*$^{-/-}$ Imm_T_{FH} cells as well as Tcf1/Lef1-deficient Inf_T_{FH} cells (Fig. 2 *A* and *B* and *SI Appendix*, Fig. S3*D*). Notably, *Prdm1*, which encodes the Blimp1 transcription factor and is derepressed in Tcf1/Lef1-deficient Inf_T_{FH} cells (16–18), remained unperturbed in *Tcf7*$^{-/-}$*Lef1*$^{-/-}$ Imm_T_{FH} cells (*SI Appendix*, Fig. S4*A*). In contrast, *Clta4*, *Fasl*, and a few other cytokine/chemokine receptors were uniquely up-regulated in *Tcf7*$^{-/-}$*Lef1*$^{-/-}$ Imm_T_{FH} cells (Fig. 2 *A* and *B*). Foxp1 is reported to induce CTLA4 expression in T_{FH} cells (28), but *Foxp1* transcripts were not significantly altered between WT and *Tcf7*$^{-/-}$*Lef1*$^{-/-}$ Imm_T_{FH} cells (*SI Appendix*, Fig. S4*A*). The increased expression of CTLA4 and LAG3 in Tcf1/Lef1-deficient Imm_T_{FH} cells was validated on the protein level (Fig. 2*C*). These observations suggest that Tcf1 and Lef1 regulate common, as well as distinct, targets in Imm_T_{FH} and Inf_T_{FH} cells. It is also noteworthy that Tcf1/Lef1-deficient non-T_{FH} cells also showed elevated expression of CTLA4 and LAG3 (*SI Appendix*, Fig. S4*B*), suggesting a conserved function of Tcf1 and Lef1 in suppressing the coinhibitory pathways in immunization-activated T cells. Because of the lack of CXCR5 expression in non-T_{FH} cells, and hence their limited access to follicle and B cells, the elevated expression of coinhibitory receptors in non-T_{FH} cells may not contribute substantially to modulating B cell functions. We therefore focused our functional and mechanistic analyses on T_{FH} cells in this work.

CTLA4 and LAG3 Blockade Rectifies B-Cell Help Defects by Tcf1/Lef1-Deficient T_{FH} Cells. Because T_{FR} cells are thymus derived (29), the adoptively transferred mature Smarta CD4^{+} T cells did not give rise to T_{FR} cells, as confirmed by the absence of *Foxp3* transcripts on RNA-seq and Foxp3 protein by intracellular staining in Smarta cells (*SI Appendix*, Fig. S4 *A* and *C*). In addition, the endogenous T_{FR} response did not develop in *Bcl6*$^{-/-}$ recipients in our experimental system. We therefore hypothesized that the impaired GC-B cell responses in recipients of *Tcf7*$^{-/-}$*Lef1*$^{-/-}$ cells were due to intrinsic effects of aberrantly induced CTLA4 and/or LAG3 on *Tcf7*$^{-/-}$*Lef1*$^{-/-}$ T_{FH} cells. Blocking the coinhibitory receptors is an effective approach to rectify T cell dysfunction (3), and in fact, treatment with CTLA4 antibodies enhances GC-B cell responses (6, 9). We thus tested treatment with anti-CTLA4 and/or anti-LAG3 in our adoptive transfer and KLH-GP61 immunization experimental system (Fig. 3*A*). When measured on day 5 postimmunization, WT and *Tcf7*$^{-/-}$*Lef1*$^{-/-}$ T_{FH} cells showed only a marginal increase in numbers by a single antibody treatment but were elevated approximately threefold by treatment with both antibodies (*SI Appendix*, Fig. S5*A*), with Bcl6, CTLA4, and LAG3 expression, per se, largely unaffected (*SI Appendix*, Fig. S5 *B–D*). On day 14 postimmunization, GC-B cells were not augmented in *Bcl6*$^{-/-}$ recipients of WT Smarta cells by anti-CTLA4/LAG3 treatment; in contrast, the reduced GC-B cell production in *Bcl6*$^{-/-}$ recipients of *Tcf7*$^{-/-}$*Lef1*$^{-/-}$ Smarta cells was potently rectified by the combination therapy (Fig. 3 *B* and *C*). In addition, GC formation and KLH-specific antibody production were substantially restored in *Tcf7*$^{-/-}$*Lef1*$^{-/-}$ recipients (Fig. 3 *D–F*). It is of note that treatment with anti-CTLA4 alone also partly restored GC-B cell formation and KLH antibody production (Fig. 3 *B*, *C*, and *F*), albeit it did not increase *Tcf7*$^{-/-}$*Lef1*$^{-/-}$ T_{FH} cell number (*SI Appendix*, Fig. S5*A*). These data indicate that blocking the coinhibitory pathways was sufficient to rectify B-cell help defects by Tcf1/Lef1-deficient T_{FH} cells and indicate that a major function of Tcf1 and Lef1 TFs in Imm_T_{FH} cells is to prevent aberrant induction of CTLA4 and LAG3.

Tcf1 and Lef1 Restrain Chromatin Accessibility at the Coinhibitory Receptor Gene Loci. To determine the mechanisms underlying Tcf1/Lef1-mediated regulation of Imm_T_{FH} cells, we used Cleavage Under Targets and Release Using Nuclease (CUT&RUN) to map global Tcf1-binding events in WT T_{FH} cells and assay for transposase-accessible chromatin with high-throughput sequencing (ATAC-seq) to compare chromatin accessibility (ChrAcc) between WT and *Tcf7*$^{-/-}$*Lef1*$^{-/-}$ T_{FH} cells. Using $P < 10^{-4}$ as a stringent cutoff in the Genrich algorithm, coupled with peak calling using model-based analysis of ChIP-seq version 2.0 (MACS2), a total of 21,602 Tcf1-binding peaks were identified in WT Imm_T_{FH} cells. Taking a gene-centric approach with a focus on the differentially expressed genes (DEGs), Tcf1 peaks were found in promoter regions (defined as +/−3 kb flanking transcription start site (TSS)) of 85% down-regulated and 78% up-regulated genes in *Tcf7*$^{-/-}$*Lef1*$^{-/-}$ T_{FH} cells, as well as in distal regulatory regions (defined as gene body and its +/−50 kb flanking sequences) at even higher percentage of these DEGs (*SI Appendix*, Fig. S6*A*). In addition, ∼82% of Tcf1 peaks overlapped with ChrAcc sites, as determined by ATAC-seq in WT T_{FH} cells (*SI Appendix*, Fig. S6*B*), consistent with previous reports (30, 31). A comparison between ATAC-seq peaks between WT and *Tcf7*$^{-/-}$*Lef1*$^{-/-}$ T_{FH} cells revealed consistent and extensive ChrAcc changes upon loss of Tcf1 and Lef1, with ∼22 and 19% of sites showing increased and decreased ChrAcc in *Tcf7*$^{-/-}$*Lef1*$^{-/-}$ T_{FH} cells, respectively (Fig. 4*A* and *SI Appendix*, Fig. S6*C*).

A focused analysis of DEG-associated ChrAcc sites showed that most ChrAcc changes, at either promoters or distal regulatory regions, were concordant with gene expression changes (Fig. 4*B*). Among the 157 up-regulated genes in *Tcf7*$^{-/-}$*Lef1*$^{-/-}$

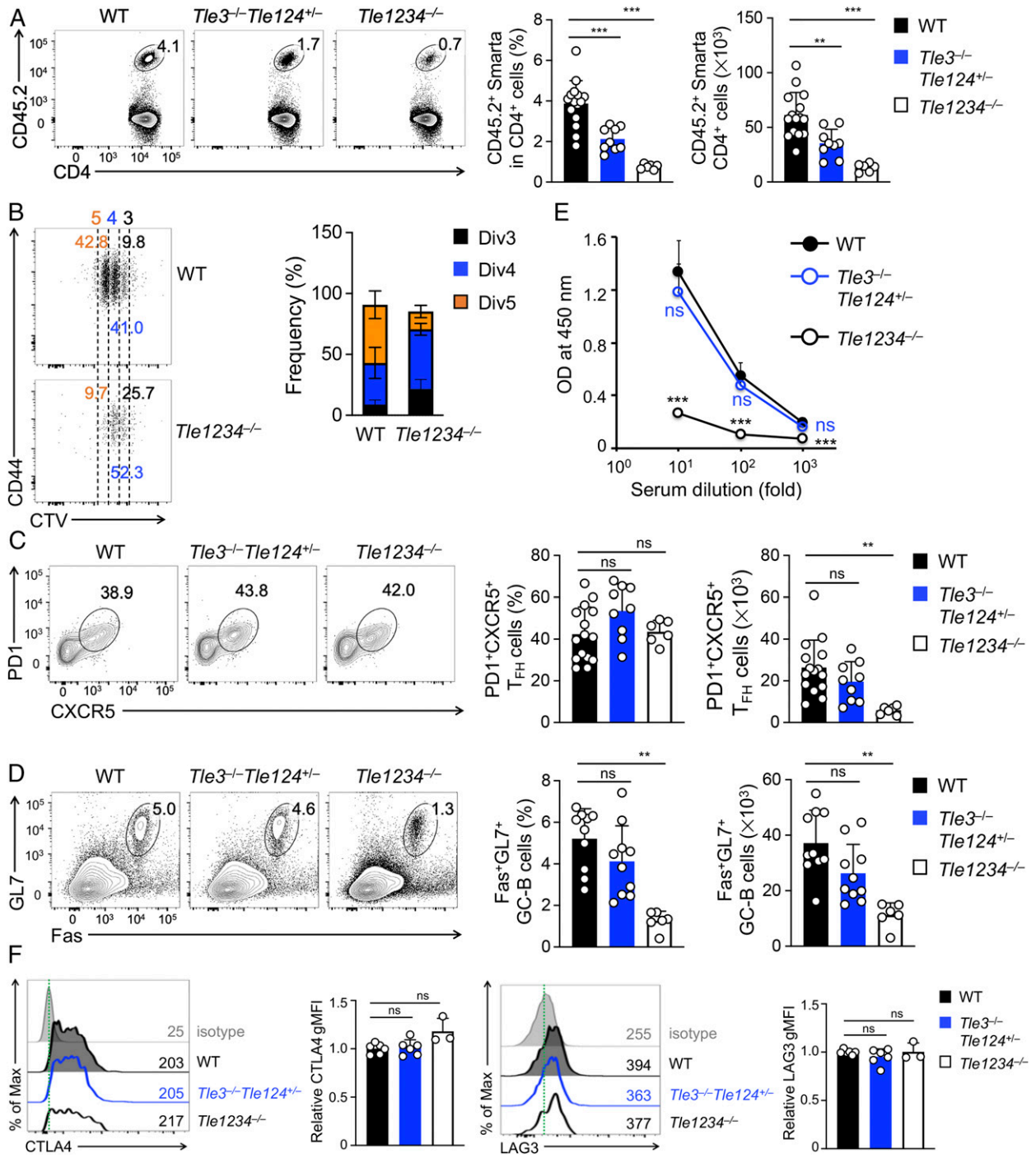

Fig. 6. Tle corepressors are highly redundant in sustaining T_{FH} cell expansion and B-cell help. (*A*) Detection of CD45.2$^+$ Smarta CD4$^+$ T cell expansion. WT, *Tle3*$^{-/-}$*Tle124*$^{+/-}$, and *Tle1234*$^{-/-}$ (1×10^5 each) Smarta CD4$^+$ T cells were adoptively transferred and recipients immunized as in Fig. 1*A*. On day 5 post-immunization, CD45.2$^+$GFP$^+$ Smarta cells were detected in TCRβ^+CD4$^+$ cells from dLNs. Representative contour plots (*Left*) are from two to three independent experiments, and cumulative data on Smarta cell frequency and numbers (*Right*) are means ± SD. (*B*) The detection of CD4$^+$ T cell activation and early division. WT or *Tle1234*$^{-/-}$ Smarta CD4$^+$ T cells were labeled with cell trace violet (CTV) and adoptively transferred at 2×10^6 cells/recipient, followed by intravenous infection with LCMV-Armstrong. CD45.2$^+$Smarta CD4$^+$ T cells were identified in the recipient spleens and assessed for CD44 expression (as an activation marker) and CTV dilution 60 h later. Representative dot plots (*Left*) show the frequency of cells in third to fifth divisions, and cumulative data from two experiments are shown in stacked bar graphs (*Right*). (*C*) The detection of CXCR5$^+$PD1$^+$ T_{FH} cells in CD45.2$^+$GFP$^+$ Smarta CD4$^+$ T cells on day 5 post-immunization. Representative contour plots (*Left*) are from two to three independent experiments, and cumulative data on T_{FH} cell frequency and numbers (*Right*) are means ± SD. (*D*) The detection of GC-B cells in *Bcl6*$^{-/-}$ recipients on day 14 postimmunization. Representative contour plots (*Left*) show percentages of GC-B cells in B220$^+$CD19$^+$ B cells in dLNs from two to three independent experiments, and cumulative data on GC-B cells (*Right*) are means ± SD. (*E*) The detection of KLH-specific IgG in sera of *Bcl6*$^{-/-}$ recipients on day 14 postimmunization. Data are from two experiments ($n = 5$ to 6). OD450, optical density at 450 nm. (*F*) The detection of CTLA4 and LAG3 proteins in *Tle*-targeted T_{FH} cells on day 5 postimmunization. In half-stacked histographs, the dotted vertical lines mark signal strength by isotype staining, and values denote geometric mean fluorescence intensity (gMFI). The bar graphs are means ± SD of relative gMFI from two experiments. $^{**}P < 0.01$; $^{***}P < 0.001$; ns, not statistically significant.

T_{FH} cells, 37 gene promoters showed increased ChrAcc (Fig. 4*C* and *SI Appendix*, Fig. S6*D*), as observed near the TSS of *Lag3* (Fig. 4*D*). In addition, 92 genes had increased ChrAcc sites in distal regulatory regions in *Tcf7*$^{-/-}$*Lef1*$^{-/-}$ T_{FH} cells (Fig. 4*E* and *SI Appendix*, Fig. S6*D*), as seen in both upstream and downstream sites flanking *Ctla4*, and upstream sites of *Fasl* (Fig. 4*D*). By stratifying with Tcf1 peaks, a substantial portion of the increased ChrAcc sites were bound by Tcf1, such as the *Lag3* promoter and some distal sites to *Ctla4* and *Fasl* (Fig. 4 *C*–*E* and *SI Appendix*, Fig. S6*D*). These observations suggest that a major function of Tcf1 and Lef1 is to restrain the ChrAcc open state to suppress coinhibitory receptor expression in Imm_T_{FH} cells.

Among the 359 down-regulated genes in *Tcf7*$^{-/-}$*Lef1*$^{-/-}$ T_{FH} cells, 46 gene promoters showed decreased ChrAcc (Fig. 5*A* and *SI Appendix*, Fig. S7*A*), as observed at the TSS of *Cxcr6* (Fig. 5*B*). In addition, 125 genes had decreased ChrAcc sites in distal regulatory regions in *Tcf7*$^{-/-}$*Lef1*$^{-/-}$ T_{FH} cells (Fig. 5*C* and *SI Appendix*, Fig. S7*B*), as seen in *Stim1* intron and the downstream region of *Il6st* (Fig. 5*B*). We also noticed that 45 down-regulated genes in *Tcf7*$^{-/-}$*Lef1*$^{-/-}$ T_{FH} cells were associated with increased ChrAcc sites (*SI Appendix*, Fig. S7 *B* and *C*), as seen in *Sell* intron (*SI Appendix*, Fig. S7*D*), where the increased ChrAcc sites may function as transcriptional suppressors as our recent study suggested (30). By stratifying with Tcf1 peaks, most decreased ChrAcc sites were bound by Tcf1, such as the *Cxcr6* promoter and some distal sites to *Stim1* and *Il6st* (Fig. 5*B*). When observed globally, the decreased ChrAcc sites showed more frequent overlap with Tcf1 peaks than the increased ChrAcc sites did, and this was true for both promoters and distal regions (Fig. 5*D*). Tcf1 peaks associated with the decreased ChrAcc sites were greater in peak height and narrower in peak width than those associated with the increased ChrAcc sites (Fig. 5*E*; also compare Fig. 5*B* with Fig. 4*D*). Motif analyses further showed that the Tcf/Lef motif was the most enriched in Tcf1 peaks associated with the decreased ChrAcc sites (Fig. 5*F*); in contrast, Tcf1 peaks associated with the increased ChrAcc sites harbored Stat, Ets, Runx, Irf, and Egr motifs (Fig. 5*G*). In addition, the canonical *Tcf/Lef* motif (TCAAAG) was found in 16.3% of Tcf1 peaks associated with decreased ChrAcc (Fig. 5 *A* and *C*) but in only 8.7% of Tcf1 peaks associated with increased ChrAcc (Fig. 4 *C* and *E* and *SI Appendix*, Fig. S7*C*). These observations suggest that for Tcf1-activated genes (i.e., down-regulated in *Tcf7*$^{-/-}$*Lef1*$^{-/-}$ T_{FH} cells), Tcf1 directly binds to these loci to maintain chromatin accessibility, while for Tcf1-repressed genes (i.e., up-regulated in *Tcf7*$^{-/-}$*Lef1*$^{-/-}$ T_{FH} cells), Tcf1 is likely recruited as a component in protein complexes to restrain chromatin accessibility.

Groucho/Tle Corepressors Are Essential for T_{FH} Cell Proliferation. To investigate how Tcf1 and Lef1 achieve negative regulation of the coinhibitory pathways in Imm_T_{FH} cells, we examined the Groucho/Tle corepressors, which are well documented to interact with Tcf/Lef TFs for transcriptional repression (22, 23). Our previous analysis of *Tle1*, *3*, and *4* deficiency in thymic development revealed strong functional redundancy and gene dosage dependency among Tle genes, with ablating *Tle3* showing stronger effect than ablating *Tle1* and/or *Tle4* (24). To fully address the redundancy issue, we conditionally targeted *Tle2* (*SI Appendix*, Fig. S8 *A* and *B*), generated Smarta^{+}*Rosa26*^{GFP} *hCD2-Cre*$^{+}$ *Tle1*-, *2*-, *3*-, and *4*-floxed mice, and investigated their roles in T_{FH} cells using adoptive transfer and the KLH-GP61 immunization approach. Deleting one allele of each Tle gene (*Tle1*$^{FL/+}$*Tle2*$^{FL/+}$*Tle3*$^{FL/+}$*Tle4*$^{FL/+}$, i.e., *Tle1234*$^{+/-}$) or both alleles of *Tle1*, *2*, and *4* along with one allele of *Tle3* (*Tle1*$^{FL/FL}$*Tle2*$^{FL/FL}$*Tle3*$^{FL/+}$*Tle4*$^{FL/FL}$, i.e., *Tle124*$^{-/-}$*Tle3*$^{+/-}$) did not affect CD4^{+} T cell expansion in response to protein immunization (*SI Appendix*, Fig. S8*C*). Ablation of all four Tle proteins (*Tle1*$^{FL/FL}$*Tle2*$^{FL/FL}$*Tle3*$^{FL/FL}$*Tle4*$^{FL/FL}$, i.e., *Tle1234*$^{-/-}$), however, greatly diminished the expansion of Smarta CD4^{+} T cells (Fig. 6*A*). On the other hand, ablation of *Tle3* together with one allele of *Tle1*, *2*, and *4* (*Tle1*$^{FL/+}$*Tle2*$^{FL/+}$*Tle3*$^{FL/FL}$*Tle4*$^{FL/+}$, i.e., *Tle3*$^{-/-}$*Tle124*$^{+/-}$) alleviated the expansion defects observed with *Tle1234*$^{-/-}$ cells (Fig. 6*A*). The defective proliferation of *Tle1234*-deficient CD4^{+} T cells was also validated when they were activated by acute viral infection and was observed at the early division stage (Fig. 6*B*).

Despite the limited expansion, the activated *Tle3*$^{-/-}$*Tle124*$^{+/-}$ or *Tle1234*$^{-/-}$ CD4^{+} T cells exhibited similar frequency of CXCR5^{+}PD1^{+} T_{FH} cells as WT cells (Fig. 6*C*), or even higher frequency of CXCR5^{+}Bcl6^{+} GC-T_{FH} cells on day 5 after immunization (*SI Appendix*, Fig. S8*D*), suggesting that Tle proteins are not necessary for activated CD4^{+} T cells to differentiate to the T_{FH} lineage. Whereas the numbers of *Tle3*$^{-/-}$*Tle124*$^{+/-}$ and WT CXCR5^{+}PD1^{+} T_{FH} or GC-T_{FH} cells were not significantly different, the counts of *Tle1234*$^{-/-}$ T_{FH} or GC-T_{FH} cells were greatly diminished (Fig. 6*C* and *SI Appendix*, Fig. S8*D*). Consistent with numerical changes in Imm_T_{FH} cells, *Bcl6*$^{-/-}$ recipients of *Tle1234*$^{-/-}$ cells but not those of *Tle3*$^{-/-}$*Tle124*$^{+/-}$ cells showed diminished GC-B cells and failed to produce KLH-specific antibodies (Fig. 6 *D* and *E*). However, neither *Tle3*$^{-/-}$*Tle124*$^{+/-}$ nor *Tle1234*$^{-/-}$ T_{FH} cells exhibited elevated expression of CTLA4 or LAG3 (Fig. 6*F*). Taken together, these observations suggest that *Tle* genes are highly redundant in regulating proliferative capacity of activated CD4^{+} T cells, likely due to gene duplication during evolution to guard this important function. As a result, *Tle* corepressors are required for T_{FH} cell expansion, albeit such a requirement does not involve negative regulation of coinhibitory receptors in cooperation with Tcf/Lef TFs.

Tcf1/Lef1-Mediated *Ctla4* Repression Requires Their Intrinsic HDAC Activity. Tcf1 and Lef1 TFs have the unusual capacity to modify histones by deacetylation, and this activity is critical for suppressing CD4^{+} lineage-associated genes in CD8^{+} single-positive thymocytes (25). To investigate if Tcf1 HDAC activity contributes to broader T cell activities, we used the CRISPR/Cas9 technique to mutate five amino acids in germline (called *Tcf7*^{M} allele herein, Fig. 7*A*). These five amino acids show a high degree of conservation between Tcf1/Lef1 HDAC domains and conventional HDAC domains, and mutating these amino acids compromised Tcf1/Lef1 HDAC activity (25) but did not detectably affect Tcf1 protein expression levels (Fig. 7*B*). To exclude compensatory effects by Lef1-derived HDAC activity, we generated Smarta^{+}*hCD2-Cre*$^{+}$*Tcf7*$^{M/M}$*Lef1*$^{FL/FL}$ (*Tcf7*$^{M/M}$*Lef1*$^{-/-}$) mice. Because the *Tcf7*^{M} allele was generated in germline, to avoid a potential impact of *Tcf7*$^{M/M}$ mutation on thymic development (to be reported elsewhere) and achieve conditional expression of Tcf1 HDAC mutant protein, we generated Smarta^{+}*hCD2-Cre*$^{+}$*Tcf7*$^{M/FL}$*Lef1*$^{FL/FL}$ (*Tcf7*$^{M/-}$*Lef1*$^{-/-}$) mice. Smarta^{+}CD4^{+} T cells from both mutant strains or WT controls were adoptively transferred into congenic mice, followed by KLH-GP61 immunization, as in Fig. 1*A*. Both *Tcf7*$^{M/M}$*Lef1*$^{-/-}$ and *Tcf7*$^{M/-}$*Lef1*$^{-/-}$ Smarta cells gave rise to similar numbers of CXCR5^{+}PD1^{+} T_{FH} and CXCR5^{+}Bcl6^{+} GC-T_{FH} cells on day 5 postimmunization as in WT Smarta cells, albeit both populations were detected at a modestly higher frequency in *Tcf7*$^{M/M}$*Lef1*$^{-/-}$ or *Tcf7*$^{M/-}$*Lef1*$^{-/-}$ cells (Fig. 7 *C* and *D*). Whereas Bcl6 and LAG3 expression was similar among WT (*Tcf7*$^{M/M}$*Lef1*$^{-/-}$ and *Tcf7*$^{M/-}$*Lef1*$^{-/-}$ T_{FH} cells), CTLA4 expression was evidently elevated in *Tcf7*$^{M/M}$*Lef1*$^{-/-}$ and *Tcf7*$^{M/-}$*Lef1*$^{-/-}$ T_{FH} cells (Fig. 7 *D* and *E*), albeit the elevated CTLA4 expression was not as profound as that in *Tcf7*$^{-/-}$*Lef1*$^{-/-}$ T_{FH} cells. Given the similar impact on T_{FH} cells between *Tcf7*$^{M/M}$*Lef1*$^{-/-}$ and *Tcf7*$^{M/-}$*Lef1*$^{-/-}$ mutations, we transferred the latter into *Bcl6*$^{-/-}$ recipients. On day 14 postimmunization, generations of GC-B cells and production of KLH-specific

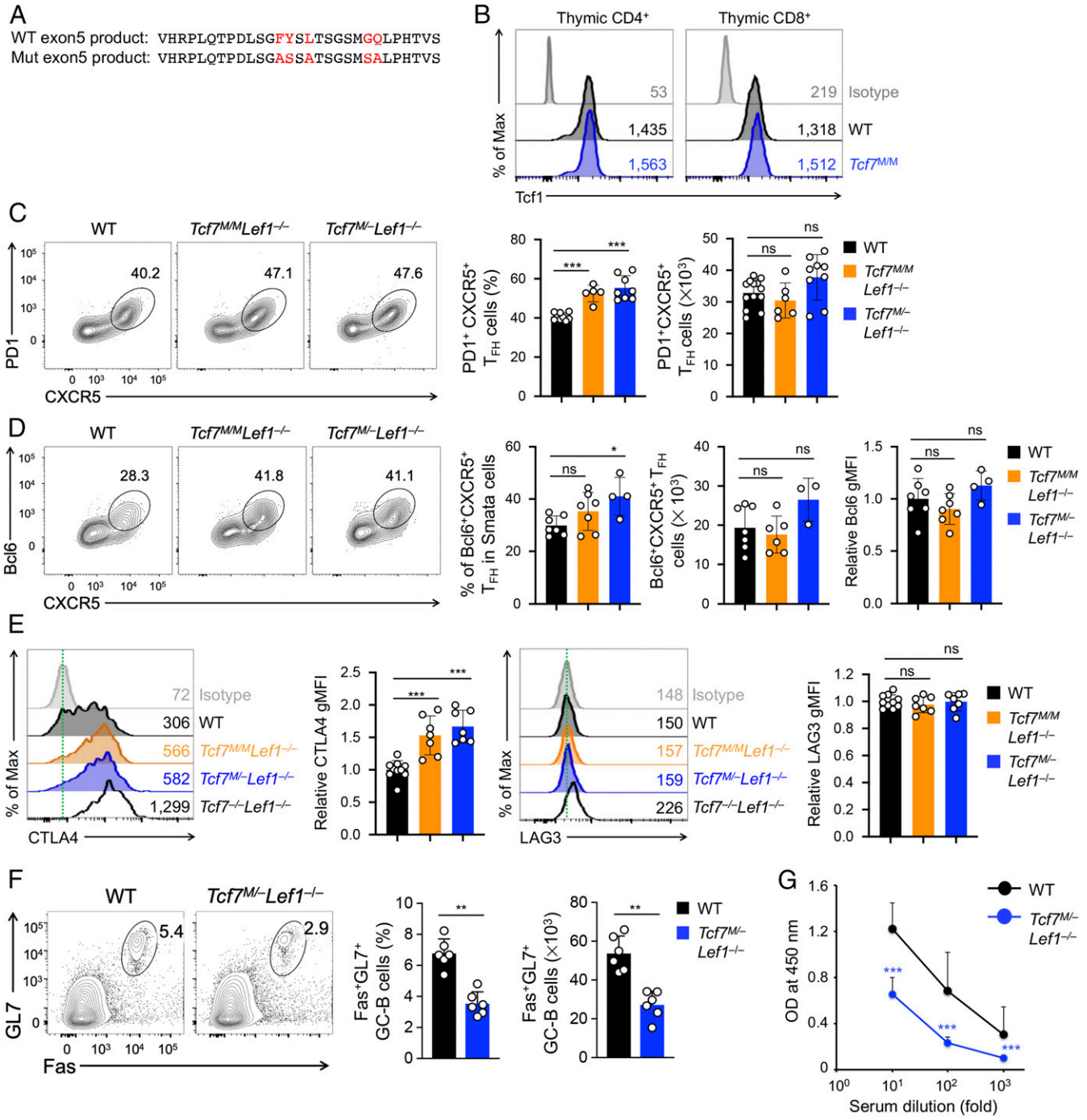

Fig. 7. Tcf1 HDAC activity is necessary for restraining CTLA4 expression in T_{FH} cells. (*A*) Alignment of WT and mutant peptide sequences derived from *Tcf7* exon 5. Highlighted in red are the five amino acids conserved between Tcf1/Lef1 HDAC domains and conventional HDAC domains (*Top*) and corresponding mutations (*Bottom*) by CRISPR-mediated exon 5 editing. (*B*) The detection of Tcf1 protein expression levels. Thymocytes were collected from WT or $Tcf7^{M/M}$ mice, and TCRβ$^+$CD4$^+$ or TCRβ$^+$CD8$^+$ thymocytes were intracellularly stained for Tcf1 expression. Representative half-stacked histograms are from two independent experiments, and values denote geometric mean fluorescence intensity (gMFI). (*C* and *D*) The detection of CXCR5$^+$PD1$^+$ (*C*) and CXCR5$^+$Bcl6$^+$ (*D*) T_{FH} cells. WT, $Tcf7^{M/M}Lef1^{-/-}$, and $Tcf7^{M/-}Lef1^{-/-}$ Smarta CD4$^+$ T cells were adoptively transferred into CD45.1$^+$ WT B6.SJL recipients, which were immunized with KLH-GP61 24 h later. On day 5 postimmunization, PD1 and Bcl6 were detected in CD45.2$^+$CXCR5$^+$ Smarta cells in dLNs. Representative contour plots are from two to four independent experiments (*Left*) and cumulative data on T_{FH} cell frequency and numbers (*Right*) are means ± SD. In *D*, the relative Bcl6 expression is shown. (*E*) The detection of CTLA4 and LAG3 proteins in Tcf1 HDAC-mutant T_{FH} cells on day 5 postimmunization. In half-stacked histographs, the dotted vertical lines mark signal strength by isotype staining, and values denote gMFI. Bar graphs are means ± SD of relative gMFI from three to five experiments. (*F*) The detection of GC-B cells in $Bcl6^{-/-}$ recipients on day 14 after immunizing the recipients of WT or $Tcf7^{M/-}Lef1^{-/-}$ Smarta CD4$^+$ T cells. Representative contour plots show percentages of GC-B cells in B220$^+$CD19$^+$ B cells in dLNs from two experiments, and cumulative data on percentages and numbers of GC-B cells are means ± SD. (*G*) The detection of KLH-specific IgG in sera of $Bcl6^{-/-}$ recipients on day 14 after immunizing the recipients of WT or $Tcf7^{M/-}Lef1^{-/-}$ Smarta CD4$^+$ T cells. Data are from three experiments ($n = 9$). OD450, optical density at 450 nm. *$P < 0.05$; **$P < 0.01$; ***$P < 0.001$; ns, not statistically significant.

antibodies were compromised in *Bcl6*$^{-/-}$ recipients of *Tcf7*$^{M/-}$ *Lef1*$^{-/-}$ cells (Fig. 7 *F* and *G*). Collectively, these findings support a direct role of Tcf1 HDAC activity in restraining CTLA4 expression in T_{FH} cells and thus guarding critical T_{FH} functions in helping B cells.

Discussion

The coinhibitory pathways are critical for preventing overexuberant immune responses. CTLA4 is deployed by multiple cell types including T_{FH}, T_{REG}, and T_{FR} cells to control the magnitude of humoral responses (5, 8). Because of the strong immunosuppressive function by T_{REG} and T_{FR} cells, the expression of CTLA4 in T_{FH} cells must be carefully modulated to avoid excessive, undue inhibition of GC-B cell responses. A previous report showed that Foxp1 contributes to induction of CTLA4 in T_{FH} cells (9). This study identified Tcf1 and Lef1 TFs as key regulators that restrain CTLA4 and LAG3 coinhibitory receptors in T_{FH} cells elicited by protein immunization. Blocking CTLA4 alone showed marginally improved expansions of Tcf1/Lef1-deficient T_{FH} cells but showed more pronounced enhancement of GC-B cells, suggesting both cell-extrinsic and -intrinsic effects were involved. In addition, blocking both CTLA4 and LAG3 further expanded Tcf1/Lef1-deficient T_{FH} cells and enhanced GC-B cell responses, highlighting the requirement for Tcf1 and Lef1 to mitigate excessive cell-intrinsic inhibitory signals. On the flip side, the break that Tcf1 and Lef1 put on CTLA4 and LAG3 expression could be released in autoimmune conditions to achieve therapeutic effects (32). Our observation that Tcf1 HDAC activity contributed to *Ctla4* repression makes Tcf1 a more amenable therapeutic target in pathogenic T_{FH} cells. This is because Tcf1 HADC activity shows selective sensitivity to HDAC inhibitors, such as Vorinostat and Tubacin (25).

It has been recognized that Tcf1, especially when ectopically expressed, increases chromatin accessibility to modulate target gene expression in exhausted CD8$^+$ T cells and even fibroblasts (30, 33). In line with these observations, a predominant function of Tcf1 and Lef1 in Imm_T_{FH} cells was to regulate transcriptional activation of downstream genes, at least in part through maintaining chromatin accessibility at the promoter and/or distal regulatory elements. Despite prevailing Tcf1 binding to 70 to 80% of these ChrAcc sites, we did notice that only 16% of these Tcf1 peaks had the canonical Tcf/Lef motif, which is historically defined as a Wnt-responsive element. Because Wnt-stabilized β-catenin does not have prominent roles in T lineage cells (20), Tcf1 and Lef1 may engage other cofactors for transcriptional activation, which may alter their preferred DNA sequences in T cells. Additionally, nonvertebrate Tcf ortholog binds to a GC-rich element through a separate "E-tail" domain located at the C terminus of its conventional high-mobility–group (HMG) DNA-binding domain (34). Besides direct contact with DNA elements, Tcf1 and Lef1 could be recruited to these sites by interacting with other DNA-bound TFs.

In addition to transactivation, Tcf1 and Lef1 were essential to negatively control chromatin accessibility to exert transcriptional repression, to suppress counterproductive pathways in T_{FH} cells. The Tcf1 peaks detected at the Tcf1-restrained sites were wider and lower compared with those detected at the Tcf1-opened sites; empirically, this observation suggests that Tcf1 is indirectly recruited as a component in a larger complex to the former sites. This notion is consistent with the observed requirement for Tcf1 HDAC activity, but not Tle corepressors, in suppressing CTLA4 expression in Imm_T_{FH} cells. Collectively, we postulate that Tcf1 is recruited as an HDAC rather than in complex with Tle corepressors to limit accessibility to the *Ctla4* locus. We recognize that Tcf1 HDAC activity may not be the sole mechanism responsible for the transcriptional repression of the coinhibitory receptors because Tcf1 HDAC mutation did not cause induction of LAG3 and the derepression of CTLA4 was not as profound as Tcf1 null mutation. Complete elucidation of repressive means that cooperate with Tcf1 HDAC await future investigations. In T_{REG} cells, we previously found that ablating Tcf1 and Lef1, but not either factor alone, resulted in evident elevation of CTLA4 expression (14), suggesting that Tcf1/Lef1-mediated CTLA4 repression is a conserved regulatory circuit in multiple T lineage cells.

This study also revealed stark differences in the requirements for Tcf1 and Lef1 in infection- and Imm_T_{FH} cells, despite some shared downstream genes. In Inf_T_{FH} cells, the prominent roles of Tcf1 and Lef1 are in two key aspects; one is transactivation of *Bcl6* and *Icos*, and the other is repression of *Prdm1* (16–18). Bcl6 and Blimp1 are mutually antagonistic, and forced expression of Bcl6 or genetic ablation of Blimp1 in Tcf1-deficient CD4$^+$ T cells rectifies T_{FH} differentiation defects (27). In contrast, neither Bcl6 transactivation nor Blimp1 repression was perturbed in Tcf1/Lef1-deficient Imm_T_{FH} cells. Because Tcf1 and Lef1 are no longer needed to balance Bcl6 and Blimp1 expression in Imm_T_{FH} cells, their functions are dedicated to transcriptional repression of *Ctla4* and *Lag3*. This finding highlights the necessity to systematically examine molecular determinants and their functional requirements in the specific context how the T_{FH} response is activated. This has important bearings on vaccine design because vaccines are delivered as live-attenuated viruses, inactivated organisms, or protein subcomponents via different routes (35). It remains to be elucidated why the same factors/pathways are differentially utilized in the T_{FH} program in response to infectious agents and protein immunization, although likely mechanistic insights might be acquired by examining the differences in the strength and duration of T cell receptor (TCR) stimulation, balance and kinetics of costimulatory and coinhibitory signals, and the cytokine milieu in future investigations. Nonetheless, our studies revealed a regulatory role for Tcf1 and Lef1 TFs to restrain coinhibitory receptors in T_{FH} cells and guard B-cell help function, and this essential function is mediated by limiting chromatin accessibility of key gene loci through their intrinsic HDAC activity.

Materials and Methods

Mice. C57BL/6J (B6), B6.SJL, *Bcl6*$^{FL/FL}$, CD4-Cre transgenic, and Rosa26^{GFP} mice were from the Jackson Laboratory. *Tcf7*$^{FL/FL}$, *Lef1*$^{FL/FL}$, *Tle1*$^{FL/FL}$, *Tle3*$^{FL/FL}$, and *Tle4*$^{FL/FL}$ mice were previously described (24, 36–39); Tcf1 HDAC mutant and *Tle2*-floxed mice were generated in this study and hCD2-Cre mice were provided by Paul E. Love (National Institute of Child Health and Human Development, NIH). All compound mouse strains used in this work were from in-house breeding at the animal care facilities of University of Iowa and Center for Discovery and Innovation, Hackensack University Medical Center. All mice analyzed were 6 to 12 wk of age, and both genders were used without randomization or blinding. All mouse experiments were performed under protocols approved by the Institutional Animal Use and Care Committees of the University of Iowa and Center for Discovery and Innovation, Hackensack University Medical Center.

Data Availability. RNA-seq, ATAC-seq, and Tcf1 CUT&RUN were performed and analyzed as detailed in *SI Appendix, Supplementary Methods*. All of the NextGen sequencing data are deposited at the Gene Expression Omnibus under the SuperSeries GSE146428 (40).

ACKNOWLEDGMENTS. We thank Drs. Thomas J. Waldschmidt (University of Iowa) and Shane Crotty (La Jolla Institute) for scientific input, the University of Iowa Flow Cytometry Core facility (J. Fishbaugh, H. Vignes, and G. Rasmussen) for cell sorting, and the University of Iowa Central Microscopy Research Facility (J. Shao) for immunofluorescence imaging. This study is supported, in part, by grants from the NIH (AI112579, AI121080, and AI139874 to H.-H.X. and P30 CA16056-42 to J.W.) and the Veteran Affairs Biomedical Laboratory Research and Development Merit Review Program (BX002903 to H.-H.X.). F.L. is supported, in part, by the National Natural Science Foundation of China (31801222, 32070888, and 82022031).

1. F. A. Schildberg, S. R. Klein, G. J. Freeman, A. H. Sharpe, Coinhibitory pathways in the B7-CD28 ligand-receptor family. *Immunity* **44**, 955–972 (2016).
2. Q. Zhang, D. A. Vignali, Co-stimulatory and co-inhibitory pathways in autoimmunity. *Immunity* **44**, 1034–1051 (2016).
3. M. K. Callahan, M. A. Postow, J. D. Wolchok, T. Targeting, Targeting T cell co-receptors for cancer therapy. *Immunity* **44**, 1069–1078 (2016).
4. J. Attanasio, E. J. Wherry, Costimulatory and coinhibitory receptor pathways in infectious disease. *Immunity* **44**, 1052–1068 (2016).
5. P. T. Sage, A. M. Paterson, S. B. Lovitch, A. H. Sharpe, The coinhibitory receptor CTLA-4 controls B cell responses by modulating T follicular helper, T follicular regulatory, and T regulatory cells. *Immunity* **41**, 1026–1039 (2014).
6. C. J. Wang *et al*., CTLA-4 controls follicular helper T-cell differentiation by regulating the strength of CD28 engagement. *Proc. Natl. Acad. Sci. U.S.A.* **112**, 524–529 (2015).
7. L. S. Walker *et al*., Established T cell-driven germinal center B cell proliferation is independent of CD28 signaling but is tightly regulated through CTLA-4. *J. Immunol.* **170**, 91–98 (2003).
8. J. B. Wing, W. Ise, T. Kurosaki, S. Sakaguchi, Regulatory T cells control antigen-specific expansion of Tfh cell number and humoral immune responses via the coreceptor CTLA-4. *Immunity* **41**, 1013–1025 (2014).
9. B. Shi *et al*., Foxp1 negatively regulates T follicular helper cell differentiation and germinal center responses by controlling cell migration and CTLA-4. *J. Immunol.* **200**, 586–594 (2018).
10. F. C. Steinke, H. H. Xue, From inception to output, Tcf1 and Lef1 safeguard development of T cells and innate immune cells. *Immunol. Res.* **59**, 45–55 (2014).
11. D. Raghu, H. H. Xue, L. A. Mielke, Control of lymphocyte fate, infection, and tumor immunity by TCF-1. *Trends Immunol.* **40**, 1149–1162 (2019).
12. J. Zhang *et al*., TCF-1 inhibits IL-17 gene expression to restrain Th17 immunity in a stage-specific manner. *J. Immunol.* **200**, 3397–3406 (2018).
13. Q. Yu *et al*., T cell factor 1 initiates the T helper type 2 fate by inducing the transcription factor GATA-3 and repressing interferon-gamma. *Nat. Immunol.* **10**, 992–999 (2009).
14. S. Xing *et al*., Tcf1 and Lef1 are required for the immunosuppressive function of regulatory T cells. *J. Exp. Med.* **216**, 847–866 (2019).
15. B. H. Yang *et al*., TCF1 and LEF1 control Treg competitive survival and Tfr development to prevent autoimmune diseases. *Cell Rep.* **27**, 3629–3645 (2019).
16. L. Xu *et al*., The transcription factor TCF-1 initiates the differentiation of T(FH) cells during acute viral infection. *Nat. Immunol.* **16**, 991–999 (2015).
17. Y. S. Choi *et al*., LEF-1 and TCF-1 orchestrate T(FH) differentiation by regulating differentiation circuits upstream of the transcriptional repressor Bcl6. *Nat. Immunol.* **16**, 980–990 (2015).
18. T. Wu *et al*., TCF1 is required for the T follicular helper cell response to viral infection. *Cell Rep.* **12**, 2099–2110 (2015).
19. J. A. Gullicksrud *et al*., Differential requirements for Tcf1 long isoforms in $CD8^+$ and $CD4^+$ T cell responses to acute viral infection. *J. Immunol.* **199**, 911–919 (2017).
20. X. Zhao *et al*., β-catenin and γ-catenin are dispensable for T lymphocytes and AML leukemic stem cells. *eLife* **9**, e55360 (2020).
21. F. Li *et al*., Ezh2 programs T_{FH} differentiation by integrating phosphorylation-dependent activation of Bcl6 and polycomb-dependent repression of p19Arf. *Nat. Commun.* **9**, 5452 (2018).
22. H. Brantjes, J. Roose, M. van De Wetering, H. Clevers, All Tcf HMG box transcription factors interact with Groucho-related co-repressors. *Nucleic Acids Res.* **29**, 1410–1419 (2001).
23. M. Agarwal, P. Kumar, S. J. Mathew, The Groucho/Transducin-like enhancer of split protein family in animal development. *IUBMB Life* **67**, 472–481 (2015).
24. S. Xing *et al*., Tle corepressors are differentially partitioned to instruct $CD8^+$ T cell lineage choice and identity. *J. Exp. Med.* **215**, 2211–2226 (2018).
25. S. Xing *et al*., Tcf1 and Lef1 transcription factors establish CD8(+) T cell identity through intrinsic HDAC activity. *Nat. Immunol.* **17**, 695–703 (2016).
26. X. Zhou, H. H. Xue, Cutting edge: Generation of memory precursors and functional memory CD8+ T cells depends on T cell factor-1 and lymphoid enhancer-binding factor-1. *J. Immunol.* **189**, 2722–2726 (2012).
27. P. Shao *et al*., Cutting edge: Tcf1 instructs T follicular helper cell differentiation by repressing Blimp1 in response to acute viral infection. *J. Immunol.* **203**, 801–806 (2019).
28. H. Wang *et al*., The transcription factor Foxp1 is a critical negative regulator of the differentiation of follicular helper T cells. *Nat. Immunol.* **15**, 667–675 (2014).
29. P. T. Sage, A. H. Sharpe, T follicular regulatory cells. *Immunol. Rev.* **271**, 246–259 (2016).
30. Q. Shan *et al*., Ectopic Tcf1 expression instills a stem-like program in exhausted $CD8^+$ T cells to enhance viral and tumor immunity. *Cell. Mol. Immunol.* 10.1038/s41423-020-0436-5 (2020).
31. C. Harly *et al*., The transcription factor TCF-1 enforces commitment to the innate lymphoid cell lineage. *Nat. Immunol.* **20**, 1150–1160 (2019).
32. N. Gensous *et al*., T follicular helper cells in autoimmune disorders. *Front. Immunol.* **9**, 1637 (2018).
33. J. L. Johnson *et al*., Lineage-determining transcription factor TCF-1 initiates the epigenetic identity of T cells. *Immunity* **48**, 243–257 (2018).
34. F. A. Atcha *et al*., A unique DNA binding domain converts T-cell factors into strong Wnt effectors. *Mol. Cell. Biol.* **27**, 8352–8363 (2007).
35. P. Piot *et al*., Immunization: Vital progress, unfinished agenda. *Nature* **575**, 119–129 (2019).
36. F. C. Steinke *et al*., TCF-1 and LEF-1 act upstream of Th-POK to promote the CD4(+) T cell fate and interact with Runx3 to silence Cd4 in CD8(+) T cells. *Nat. Immunol.* **15**, 646–656 (2014).
37. S. Yu *et al*., The TCF-1 and LEF-1 transcription factors have cooperative and opposing roles in T cell development and malignancy. *Immunity* **37**, 813–826 (2012).
38. J. C. Wheat *et al*., The corepressor Tle4 is a novel regulator of murine hematopoiesis and bone development. *PLoS One* **9**, e105557 (2014).
39. S. Ramasamy *et al*., Tle1 tumor suppressor negatively regulates inflammation in vivo and modulates NF-κB inflammatory pathway. *Proc. Natl. Acad. Sci. U.S.A.* **113**, 1871–1876 (2016).
40. H. H. Xue, Tcf1 and Lef1 regulate follicular helper T cell function elicited by vaccination. *Gene Expression Omnibus*. https://www.ncbi.nlm.nih.gov/geo/query/acc.cgi?acc=GSE146428. Deposited 5 March 2020.